

# Natural Coronagraphic Observations of the Eclipsing T Tauri System KH 15D: Evidence for Accretion and Bipolar Outflow in a WTTS<sup>1</sup>

Catrina M. Hamilton<sup>2</sup> and William Herbst

*Astronomy Department, Wesleyan University, Middletown, CT 06459*

catrina@astro.wesleyan.edu, bill@astro.wesleyan.edu

Reinhard Mundt and Coryn A. L. Bailer-Jones

*Max-Planck-Institut für Astronomie, Königstuhl 17, D-69117 Heidelberg, Germany*

mundt@mpia-hd.mpg.de, calj@mpia-hd.mpg.de

and

Christopher M. Johns-Krull

*Physics and Astronomy Department, Rice University, Houston, TX 77005*

cmj@rice.edu

## ABSTRACT

We present high resolution ( $R \sim 44,000$ ) UVES spectra of the eclipsing pre-main sequence star KH 15D covering the wavelength range 4780 to 6810 Å obtained at three phases: out of eclipse, near minimum light and during egress. The system evidently acts like a natural coronagraph, enhancing the contrast relative to the continuum of hydrogen and forbidden emission lines during eclipse. At maximum light the H $\alpha$  equivalent width was  $\sim 2$  Å and the profile showed broad wings and a deep central absorption. During egress the equivalent width was much higher ( $\sim 70$  Å) and the broad wings, which extend to  $\pm 300$  km/s, were prominent. During eclipse totality the equivalent width was less than during

---

<sup>1</sup>Based on Ultraviolet-Visual Echelle Spectrograph observations collected at the European Southern Observatory's Very Large Telescope via Director's Discretionary Time, within the observing program P267.C-5736.

<sup>2</sup>Physics Department, Wesleyan University, Middletown, CT 06459

egress ( $\sim 40 \text{ \AA}$ ) and the high velocity wings were much weaker.  $H\beta$  showed a somewhat different behavior, revealing only the blue-shifted portion of the high velocity component during eclipse and egress. [OI]  $\lambda\lambda 6300, 6363$  lines are easily seen both out of eclipse and when the photosphere is obscured and exhibit little or no flux variation with eclipse phase. Our interpretation is that KH 15D, although clearly a weak-line T Tauri star by the usual criteria, is still accreting matter from a circumstellar disk, and has a well-collimated bipolar jet. As the knife-edge of the occulting matter passes across the close stellar environment it is evidently revealing structure in the magnetosphere of this pre-main sequence star with unprecedented spatial resolution. We also show that there is only a small, perhaps marginally significant, change in the velocity of the K7 star between the maximum light and egress phases probed here.

*Subject headings:* stars:individual (KH 15D) — accretion — line:profiles

## 1. Introduction

KH 15D is a unique system in which a pre-main sequence star is periodically occulted by extended, non-luminous matter, presumably part of a circumstellar disk (Herbst et al. 2002). Every 48.36 days the star fades over 2-3 days by  $\sim 3.5$  mag and remains near minimum light for  $\sim 20$  days. The eclipse duration has been increasing with time, by  $\sim 1-2$  days/yr. Hamilton et al. (2001) obtained low resolution spectra in and out of eclipse and concluded that the star was a K7 weak-line T Tauri star (WTTS). The WTTS classification, based on the equivalent width (EW) of the  $H\alpha$  line out of eclipse, is supported by the lack of any  $IR^2$  or UV excess emission and the absence of substantial photometric variability outside of eclipse. Based on its membership in NGC 2264 (Sung et al. 1997), the estimated mass of the K7 star is  $0.5-1 M_{\odot}$  and its age is 2-4 Myr.

In an attempt to learn more about this unique system we obtained high resolution spectra during the eclipse of December 2001. We hoped to determine whether KH 15D is a radial velocity variable, whether there was evidence for additional light in the system beyond that of the K7 star, and whether the occultation had any effect on the spectrum. In fact, we found dramatic changes in the line profiles of  $H\alpha$  and  $H\beta$ , as well as weak forbidden emission lines that become much more visible during eclipse. Evidently, the KH 15D system behaves like a “natural coronagraph”, allowing us to see details of its close circumstellar environment

---

<sup>2</sup>H-K = 0.14, K-L = 0.03 out-of-eclipse, K. Haisch, private communication.

during eclipse. Our evidence suggests that this WTTS is actively accreting gas and driving a bipolar outflow, although probably not at the rate of a typical CTTS. This calls into question the common practice of associating WTTS characteristics with the absence of an accretion disk.

## 2. Observations and the Absorption Spectrum

High resolution echelle spectra of KH 15D were obtained on the nights of UT 2001 Nov. 29, when it was in its bright state just prior to eclipse, on UT 2001 Dec. 14, just past mid-eclipse, and again on UT 2001 Dec. 20 during egress (see Figure 1). These data were collected with the Ultraviolet-Visual Echelle Spectrograph (UVES) on the European Southern Observatory’s Very Large Telescope (VLT), at Mount Paranal, Chile. The wavelength range is  $\sim 4780$  to  $6810$  Å. A  $50$  Å gap centered on  $5800$  Å is present due to use of the red arm which employs a mosaic of two  $4096 \times 2048$  CCDs (D’Odorico et al. 2000). With a  $1''$  slit, the spectral resolution is  $\sim 44,000$ . The spectra presented here were reduced via the UVES pipeline. Information regarding the reduction process can be found at <http://www.eso.org/instruments/uves/>. As a check on this, the spectra were also reduced in the manner described by Valenti (1994). Both procedures make use of a sky subtraction algorithm. No significant differences were found between the data reduced by these techniques and the UVES pipeline reduction is adopted here.

The UVES spectra confirm that, out of eclipse, the primary light source in the KH 15D system is a K7 WTTS. The 29 Nov. spectrum was visually compared in detail to 61 Cyg B, a typical K7 V, to look for any evidence of a second source of light in the system. No additional features were found. This spectrum was also compared to a rotationally broadened, synthetic K7 V template to determine its  $v \sin(i)$ , which we estimate to be  $< 5$  km/s. The EW of the LiI 6707 feature is  $0.401 \text{ Å} \pm 0.001$ , consistent with the value of  $0.47 \text{ Å} \pm 0.05$  measured on a low resolution spectrum by Hamilton et al. (2001).

The out-of-eclipse spectrum was cross-correlated against HD 55999, a standard observed on the same nights, to determine the radial velocity of KH 15D. This was done with the IRAF<sup>3</sup> task FXCOR. Since the spectra were obtained on two CCDs covering different wavelength regions, a cross-correlation was performed on each, avoiding the emission line

---

<sup>3</sup>Image Reduction and Analysis Facility, written and supported by the IRAF programming group at the National Optical Astronomy Observatories (NOAO) in Tucson, Arizona. NOAO is operated by the Association of Universities for Research in Astronomy (AURA), Inc. under cooperative agreement with the National Science Foundation.

regions of  $H\alpha$ , and  $H\beta$ . A heliocentric radial velocity of  $+9.0 \text{ km/s} \pm 0.2$ , was found by this procedure for KH 15D on 29 Nov 2001.

The egress spectrum was cross-correlated against the out-of-eclipse spectrum in the same manner to look for any radial velocity variation between 29 Nov. and 20 Dec. A difference in heliocentric radial velocity of  $3.3 \pm 0.6 \text{ km/s}$  was found. The radial velocity of the star on 20 Dec. was, therefore,  $+12.3 \text{ km/s} \pm 0.6$ . Whether this detection of radial velocity variation means that the K7 star is a spectroscopic binary remains to be seen. Photospheric line profile variations are expected in a partially eclipsed star and the likely importance of scattered radiation near minimum light further complicates the interpretation. Clearly a more extensive radial velocity study of the system is needed and is underway (J. Johnson & G. Marcy, private communication).

### 3. The Emission Line Spectrum

In Figures 2-4, we show the  $H\alpha$ ,  $H\beta$ , and [OI] 6300 emission-line profiles for KH 15D. Each spectrum has been flux calibrated to a relative scale using an R magnitude for the date, as given in Table 1. The quoted uncertainties on the magnitudes reflect a small degree of non-simultaneity in the spectral and photometric data as well as the need to transform from I (where the data were more numerous) to R. Since spectral and photometric data were taken within an hour of each other, except at maximum light (when the brightness is nearly constant with time) and since the color variation is quite small ( $\sim 0.1$  mag in R-I over the full brightness range), the uncertainty in R is only  $\sim 0.1$  mag. Julian dates for each observation, measured I magnitudes, derived R and V magnitudes, measured EWs, and derived  $H\alpha$  and [OI] fluxes are listed in Table 1. The EW measurements refer to the entire profile, both red- and blue-shifted components combined. On Figs. 2 and 3, the arrows indicate where HI nebular emission could have affected the profile, whereas on Fig. 4 the arrow indicates where [OI]  $\lambda 6300$  from the night sky may not have been removed completely.

Figure 2 shows that dramatic changes occurred in the  $H\alpha$  emission line profile of KH 15D during eclipse and egress. Out of eclipse, the star appears to be a WTTS with an  $\text{EW}(H\alpha) \sim 2 \text{ \AA}$ , but with a double-peaked profile, having a central absorption and faint, but clearly detectable broad wings. A comparison with the  $H\alpha$  profiles of other WTTSs (Hartmann 1982; Mundt et al. 1983; Finkenzeller & Basri 1987; Edwards et al. 1994; Reipurth et al. 1996) shows that only 3 out of 19 such stars exhibited double-peaked profiles similar to KH 15D, with UX Tau A being the most similar (see Reipurth et al. (1996)). Most WTTSs show narrow, single-peaked emission lines. It is also interesting that the central absorption feature appears to extend below the stellar continuum. This is unusual for any TTS, weak

or classical. During eclipse and egress, the “natural coronagraph” effect is clear. Near mid-eclipse, the EW of  $H\alpha$  grows to  $\sim 40 \text{ \AA}$ , while the relative flux drops by  $\sim 50\%$ . During egress the EW rises to  $\sim 70 \text{ \AA}$ , as the flux increases, exceeding even its out-of-eclipse value. In all cases, a double-peaked profile is observed. The emission line profile during mid-eclipse extends to  $\pm 200 \text{ km/s}$  with significantly less flux in the extended wings, as compared to the profile during egress, which extends to  $\pm 300 \text{ km/s}$ .

Figure 3 shows the corresponding  $H\beta$  line profiles. Again, dramatic EW and line profile changes are evident. Although the out-of-eclipse  $H\beta$  line profile is heavily affected by the underlying stellar absorption spectrum, it is similar to  $H\alpha$ . In the egress spectrum, however, the emission occurs primarily on the blue side with a wing extending to  $-300 \text{ km/s}$ . The asymmetry in this line is much more striking than  $H\alpha$ . During mid-eclipse, although little  $H\beta$  flux is present, the shape of the line profile appears similar to egress. The weak features visible in this profile at  $-25 \text{ km/s}$  are probably due to an improper background subtraction of the  $H\beta$  emission from NGC 2264.

Figure 4 shows the emission-line profiles for the [OI]  $6300 \text{ \AA}$  line. The [OI] line, which is weak, but clearly discernable at maximum light, becomes prominent at mid-eclipse and during egress. The line flux seems to be about the same out of eclipse and during egress, although slightly higher at mid-eclipse. We caution against any extreme interpretation of this measurement. The profile during mid-eclipse was disturbed by an improper background subtraction, and we feel that our errors are most likely underestimated. However, this behavior would indicate that none of the [OI] emitting zone suffers variable occultation at the phases of our observations. This is fully expected given the spatial extent of the (bipolar) forbidden line emitting regions in CTTSs. The peak of the high velocity component of the [OI] emission in typical CTTSs originates at about 30 AU from the star (Hirth et al. 1997).

The EW of the [OI]  $\lambda 6300$  line in the out-of-eclipse spectrum is about  $0.17 \text{ \AA}$ , which is quite large for a WTTS. Only one of the ten WTTSs in Table 3 of Hartigan et al. (1995) has a detectable [OI]  $\lambda 6300$  line (with an EW =  $0.5 \text{ \AA}$ ). The others have upper limits of about  $0.06 \text{ \AA}$ . Most CTTSs in that table, on the other hand, have EWs of  $0.5 - 3 \text{ \AA}$ . The profiles obtained during mid-eclipse and egress suggest that we have two emission peaks, at about  $-20$  and  $+18 \text{ km/s}$  with emission wings extending  $-60$  to  $+50 \text{ km/s}$ , respectively. These profiles are quite different from the [OI]  $\lambda 6300$  profile seen in most strong-emission CTTSs (with strong veiling), which often have a high-velocity component at  $-100$  to  $-150 \text{ km/s}$  (resulting from the jet) and a low-velocity component at about  $-20 \text{ km/s}$  (Hartigan et al. 1995; Hirth et al. 1997). In addition, the profile is quite different from that of a CTTS with small veiling and IR excess (see the bottom profile in Figure 11 of Hartigan et al. (1995)). These latter profiles are usually single-peaked and unshifted in velocity. Although

the profile shape for KH 15D is not fully clear due to imperfect subtraction of the emission of [OI] at 6300 Å in the night sky, it is most likely double-peaked. Such a profile can be most easily explained by a bipolar jet moving nearly perpendicular to the line of sight, quite consistent with our expectation that the disk associated with KH 15D is viewed nearly edge on, resulting in a very small radial velocity separation between the two jets. The profile catalog of Hartigan et al. (1995) contains several examples of bipolar jet sources (RW Aur, AS 353A, DD Tau), where the two jet components are clearly separated due to favorable inclination angles.

#### 4. Discussion

It is important to keep in mind that we do not yet know the geometry of the KH 15D system. In particular, it is not certain whether the occultation proceeds along a line perpendicular to or parallel to the rotation axis of the K7 star (or neither) or to what extent the rotation axis, the presumed stellar magnetic axis and the orbital plane are aligned. It is not even known whether, relative to the system’s center of mass, it is the K7 star or the occulting matter which is primarily in motion. Detailed modeling of the system must obviously await clarification of these basic issues. However, a preliminary qualitative interpretation of the emission line variations is possible and provided in this section.

We believe that the observed spectral variations of KH 15D can be understood qualitatively in terms of a weakly accreting, “scaled down” classical T Tauri star (see e.g., Muzerolle et al. (2001)) whose photosphere and magnetosphere are periodically occulted by a relatively sharp knife-edge (as described in Herbst et al. (2002), their Fig. 5). We expect such a star to have a bipolar jet region, which we assume, by analogy with the CTTS, is revealed by the forbidden emission line radiation. Assuming a jet velocity of 200 km/s (which is the average jet velocity for CTTSs derived by Hirth et al. (1994)) and adopting a radial velocity of  $\pm 20$  km/s for the [OI]  $\lambda 6300$  peaks, we derive an inclination angle for the jet to the line of sight of  $84^\circ$ . This is consistent with a general picture for the system in which we view the K7 star close to the orbital plane of its circumstellar (or circumbinary) disk and the jets emerge roughly perpendicular to the disk plane, as for the star associated with HH 30 and other examples imaged by the Hubble Space Telescope (Ray et al. 1996). The absence of any significant variation in the profiles or flux of the forbidden line radiation during eclipse is consistent with the expectation, based on the CTTS analogy, that it arises at distances of tens of AU’s from the star, beyond the region variably occulted.

The behavior of the hydrogen lines is complex because some components do arise close to the star and, therefore, suffer variable occultation effects along with the photosphere. Since

we expect that the  $H\alpha$  line has a much higher optical depth than the  $H\beta$  line, it is obvious that any emission line region will be more extended in  $H\alpha$  than  $H\beta$ . If we assume that the magnetic axis of the K7 star is tilted toward us at  $\sim 5\text{-}10^\circ$ , which is a reasonable assumption supported by the [OI] line profiles, at mid-eclipse, one can qualitatively understand the  $H\alpha$  line profile as resulting from low velocity material in the outer, more extended  $H\alpha$  emission region while the star and the  $H\beta$  line forming region are obscured by the occulting disk material. This would also explain why there is almost no  $H\beta$  flux during mid-eclipse. During egress, we expect most of the  $H\alpha$  emission line region, as well as some of the  $H\beta$  emission line region, which is closer to the star, to be visible. The  $H\alpha$  line profile during egress has a low velocity emission peak with a central absorption feature similar to what is seen in the out-of-eclipse profile. Additionally, two “shoulders” appear along the profile at about  $\pm 150$  km/s extending out to  $\pm 300$  km/s. These “shoulders” could be due to material rotating in the outer parts of the magnetosphere. However, given that the  $v \sin(i)$  is measured to be  $< 5$  km/s, and that the magnetosphere only extends out to about 5-6 stellar radii, the maximum rotational velocity is about 5-6  $v \sin(i)$  or 25-30 km/s, making it difficult to explain the  $H\alpha$  emission-line profile with a rotating magnetosphere.

A more attractive hypothesis is that the high velocity “shoulders” on the  $H\alpha$  line, so prominent in the egress spectrum, arise from material falling along magnetic accretion columns. This interpretation can also qualitatively account for the  $H\beta$  emission line profile during egress. Adopting values for the mass and radius of the K7 star from Table 1 of Hamilton et al. (2001), a free-fall velocity of about 380 km/s can be associated with material at the surface of the star. Since  $H\beta$  is produced much closer to the star, the blue-shifted wing extending to nearly -350 km/s could be representative of material accreting along magnetic field lines near the pole. The asymmetry seen in the  $H\beta$  emission line profile is most likely due to the fact that the star is slightly inclined toward our line of sight. The reappearance of both a blue and red wing to the  $H\alpha$  line during the early part of egress, when most of the stellar photosphere is still occulted, shows that both red-shifted and blue-shifted gas is present along the same line of sight towards the small portion of the photosphere and magnetosphere that is being uncovered first. This also supports an accretion interpretation as opposed, say, to a rotation interpretation for the high velocities.

## 5. Conclusions

It appears that KH 15D, although clearly a WTTS by the usual criteria of weak  $H\alpha$  emission, absence of UV or IR excess emission, and relative photometric stability, is still undergoing active accretion and driving a bipolar outflow. It provides a cautionary example

against assuming that all stars with WTTS characteristics no longer have accretion disks. The unique geometry of this system, in which a relatively sharp-edged occulting mask crosses the photosphere has created a “natural coronagraph” which enhances the visibility of the star’s magnetosphere during eclipse. The occultation also evidently crosses the inner portion of the star’s magnetosphere, where high velocity gas motions arise, probably from magnetically channeled accretion. Synoptic studies of this star may ultimately allow us to reconstruct aspects of the structure of its magnetosphere with spatial resolution that will be unobtainable in other objects for decades to come.

We thank U. Bastian, M. Ibraghimov, J. Johnson, G. Marcy, F. Vrba, and J. Aufdenberg for helpful conversations and useful data on this star. W.H. acknowledges support from NASA through its Origins of Solar Systems program.

## REFERENCES

- D’Odorico, S., et al. 2000, in Proc. SPIE Vol. 4005, p.121-130, ”Discoveries and Research Prospects from 8- to 10-Meter-Class Telescopes”, ed. Bergeron, J.
- Edwards, S., Hartigan, P., Ghandour, L., and Andrulis, C. 1994, AJ, 108, 1056
- Finkenzeller, U., & Basri, G. 1987, ApJ, 318, 823
- Hamilton, C.M., Herbst, W., Ferro, A.J., and Shih, C. 2001, ApJ, 554, L201
- Hartigan, P., Edwards, S., and Ghandour, L. 1995, ApJ, 452, 736
- Hartmann, L. 1982, ApJS, 48, 109
- Herbst, W., Hamilton, C.M., Vrba, F.J., Ibrimahov, M., Bailer-Jones, C.A.L., Mundt, R., et al. 2002, PASP, 114, 1167
- Hirth, G.A., Mundt, R., Solf, J, and Ray, T.P. 1994, ApJ, 427, L99
- Hirth, G.A., Mundt, R., and Solf, J. 1997, A&ASS, 126, 437
- Mundt, R., Walter, F.M., Feigelson, E.D., Finkenzeller, U., Herbig, G.H., Odell, A.P. 1983, ApJ, 269, 229
- Muzerolle, J., Calvet, N., and Hartmann, L. 2001, ApJ, 550, 944
- Ray, T.P., Mundt, R., Dyson, J.E., Falle, S.A.E.G., Raga, A.C. 1996, ApJ, 468, L103

Reipurth, B., Pedrosa, A., Lago, M.T.V.T. 1996, A&ASS, 120, 229

Sung, H., Bessel, M.S., and Lee, S. 1997, AJ, 114, 2644

Valenti, J. 1994, PhD Thesis, University of California, Berkeley

Table 1. Journal of Observations and Measurements.

JD (2452...)	V(mag)	R(mag)	I(mag)	EW <sub>(H<math>\alpha</math>)</sub> (Å)	EW <sub>(OI)</sub> (Å)	Flux <sub>(H<math>\alpha</math>)</sub> (x 10 <sup>-6</sup> ) <sup>a</sup>	Flux <sub>[OI]</sub> (x 10 <sup>-6</sup> ) <sup>a</sup>
242.7296	16.10 ± 0.02	15.27 ± 0.02	14.49 ± 0.02	2.11 ± 0.08	0.22 ± 0.04	1.6 ± 0.06	0.17 ± 0.03
257.7840	19.6 ± 0.1	18.9 ± 0.1	18.2 ± 0.1	39.3 ± 1.5	8.4 <sup>b</sup> ± 0.2	1.1 ± 0.04	0.24 ± 0.02
263.6871	19.1 ± 0.1	18.3 ± 0.1	17.6 ± 0.1	70.8 ± 5.1	3.1 ± 0.2	3.4 ± 0.24	0.15 ± 0.02

<sup>a</sup>Calculated as  $EW_{(H\alpha)} \times 10^{-0.4 \cdot R}$

<sup>b</sup>This EW was measured with the spike removed.

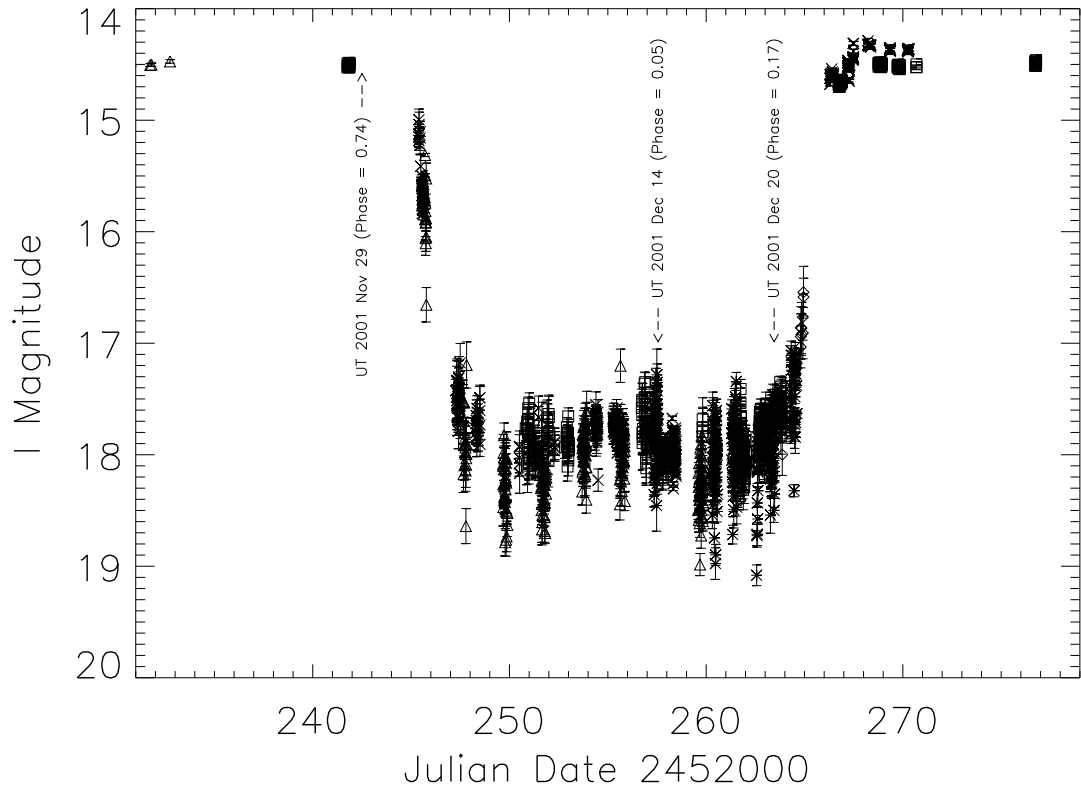


Fig. 1.— The December 2001 eclipse of KH 15D; photometry from Herbst et al. (2002). Arrows indicate epochs at which the UVES spectra were obtained.

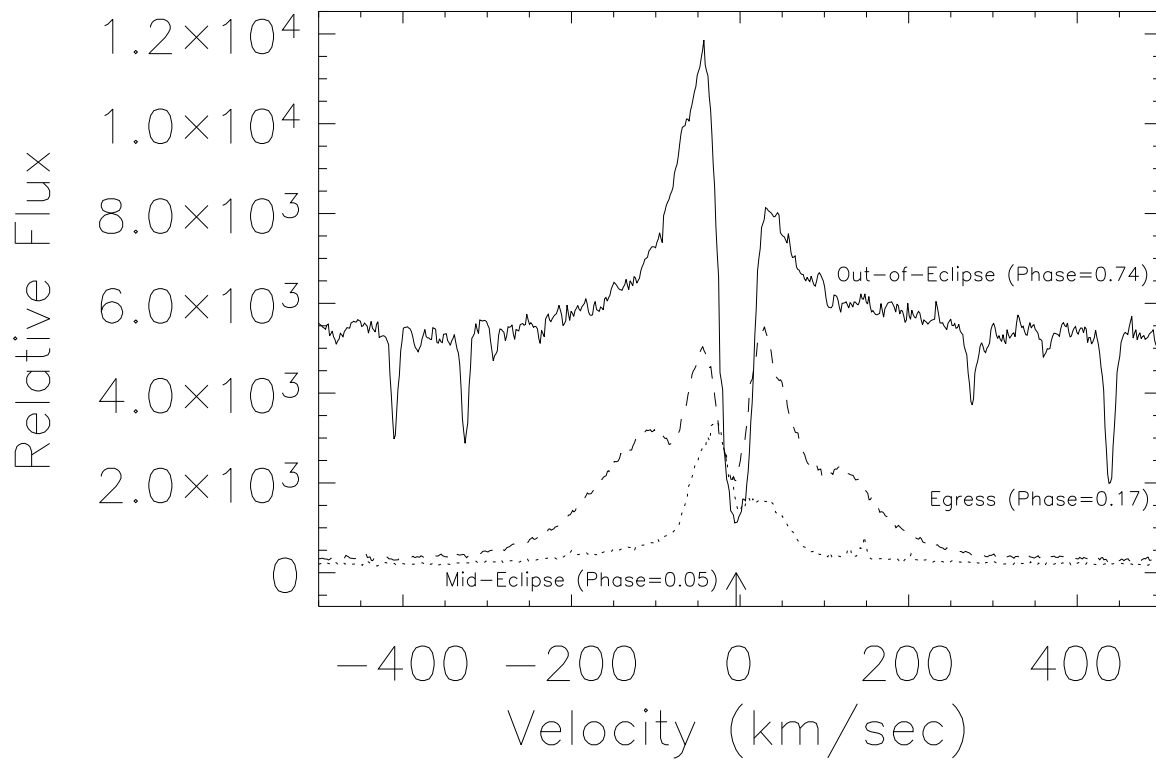


Fig. 2.— H $\alpha$  profiles of KH 15D obtained with the VLT and UVES during the December 2001 eclipse. The arrow indicates where the nebular emission of H $\alpha$  is seen in the background. The velocities are shown in the reference frame of the star.

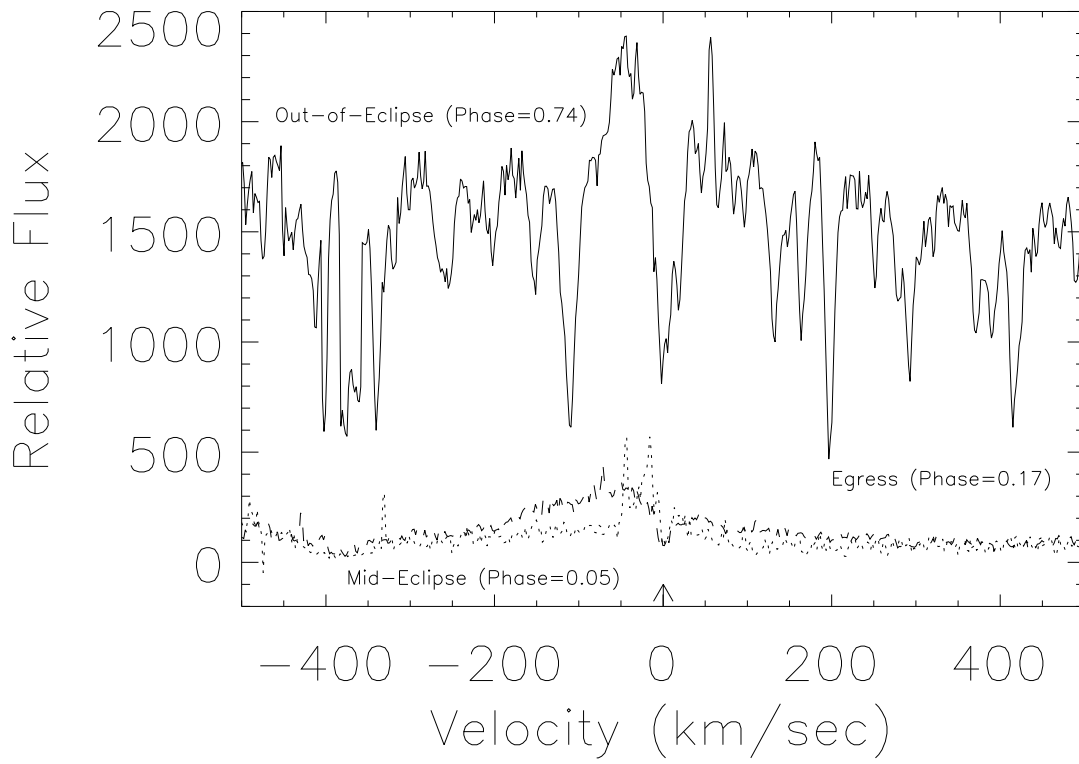


Fig. 3.—  $H\beta$  profiles of KH 15D obtained with the VLT and UVES during the December 2001 eclipse. The arrow indicates where the nebular emission of  $H\beta$  is seen in the background. The velocities are shown in the reference frame of the star.

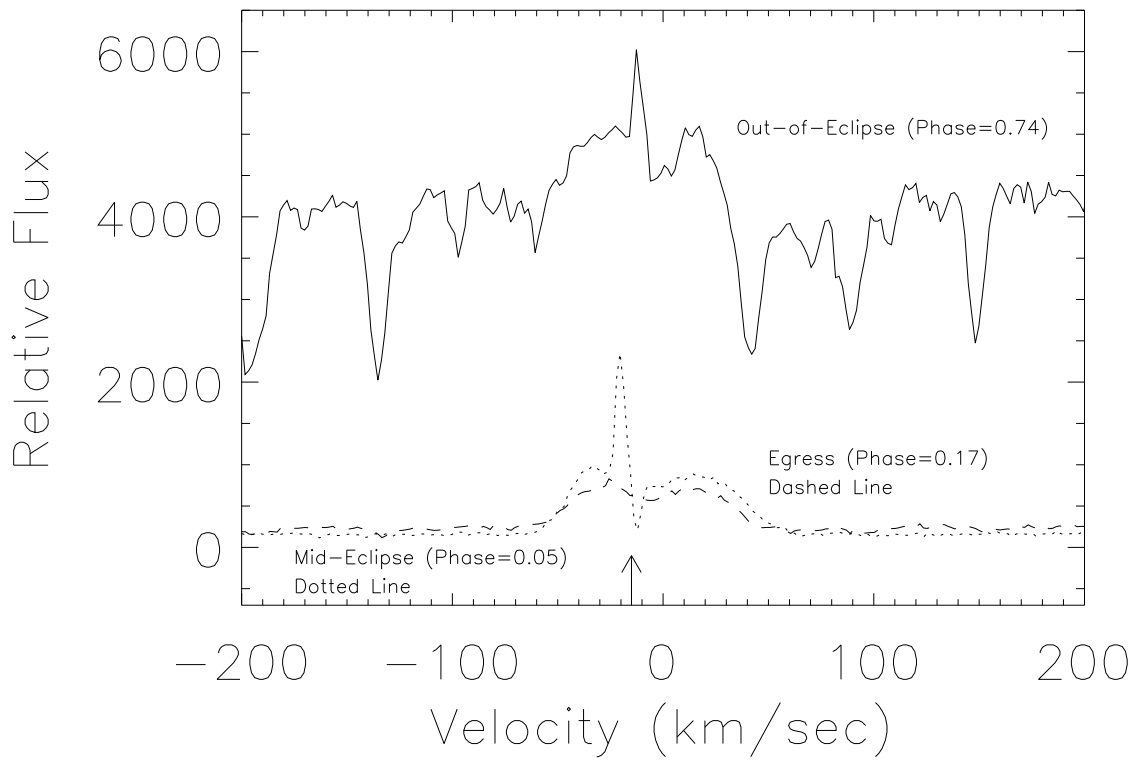


Fig. 4.— [OI] 6300 Å profiles of KH 15D obtained with the VLT and UVES during the December 2001 eclipse. The arrow indicates where the night sky emission of [OI] has not been removed completely. The velocities are shown in the reference frame of the star.